Chiroptical Properties of Some Monoazapentahelicenes

France Lebon,[†,‡] Giovanna Longhi,[†,‡] Fabrizio Gangemi,[†] Sergio Abbate,*[,†,‡] Jan Priess,[§] Markus Juza,[§] Cristina Bazzini,[||] Tullio Caronna,[||] and Andrea Mele[⊥]

Dipartimento di Scienze Biomediche e Biotecnologie, Università di Brescia, viale Europa 11, I-25123 Brescia, Italy, INFM-Istituto Nazionale di Fisica della Materia, UdR Brescia, via Valotti 9, I-25123 Brescia, Italy, CarboGen AG (Aarau), Schachenallee 29, CH-5001 Aarau, Switzerland, Facoltà di Ingegneria, Università di Bergamo, via Marconi 5,I-24044 Dalmine (BG), Italy, and Dipartimento di Chimica, Materiali ed Ingegneria Chimica "Giulio Natta", Politecnico di Milano, Via Mancinelli 7, I-20131 Milano, Italy

Received: September 24, 2004

Three closely related previously synthesized monoaza[5]helicenes have been resolved into their enantiomers via enantioselective HPLC using a cellulose-derivative Chiralcel OD column. Circular dichroism (CD) spectra of the enantiomerically enriched samples have been recorded and assigned. The spectra were analyzed as a function of time, and different rate constants were found in the kinetics of racemization for the three molecules. Ab initio DFT calculations for the ground electronic states were employed to determine minima and saddle point structures and to understand the racemization process. The theoretical geometries compared well with those from X-ray structures. CD spectra were calculated by TD-DFT ab initio methods, and compared with experimental data.

I. Introduction

Helicenes form an attractive set of molecules that, ever since they were first synthesized,[1] have stimulated the curiosity and imagination of numerous scientists, for several fundamental reasons: the synthesis, either via chemistry[1,2] or photochemistry;[3,4] the separation of enantiomers and the determination of the absolute configuration;[5,6] the study of the thermal stability of enantiomers and their path to racemization;[2] and, most important in our opinion, the challenge posed to MO theories for determining structure and interpreting spectra.[7−11]

However, recently interest in helicenes has not been merely speculative, but also applicative because these molecules have a nicely delocalized π-electron system and thus they exhibit interesting opto- and photoelectronic properties;[12,13] i.e., they are organic semiconductors. What makes these molecules special is the chirality of the π-electron system, which makes the helicene a prototypic inherently dissymmetric chromophore.[14] Undoubtedly this property also determines their unique applicative qualities. For all these reasons, we decided to study the chiroptical properties of a series of three previously synthesized monoaza[5]helicenes,[15] the chemical structures of which are reported below as **H4**, **H5**, and **H6** (where **4**, **5,** and **6** designate the atomic positions occupied by the nitrogen atom).

In ref 15, X-ray crystallographic studies were presented for the racemic mixtures; here, we will present the results of enantiomeric separation via HPLC. We will report also the CD and absorption spectra of the enantiomerically enriched samples, and make a rather thorough assignment of the observed CD bands, as results also from the comparison with the "parent" molecule, [5]helicene. An ab initio-DFT calculation will allow us to quantitatively understand the quite different enantiomeric stability observed for the three helicenes, **H4**, **H5**, and **H6**. Finally, time-dependent density functional theory (TD-DFT) calculations, which are a natural evolution of the methods first presented in ref 7, will allow a less empirical interpretation of the spectral data.

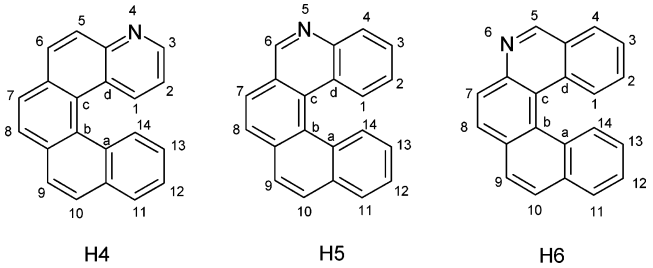

II. Experimental Methods

(a) Enantiomeric Resolution. A Merck HPLC column (type NW50) was packed with 200 g of Chiralcel OD, 20 μm particle size obtained from Chiral Technologies Europe (Strasbourg, France). The resulting column had a dimension of 185 × 48 mm ID. Preparative separations were performed with an isocratic eluent mixture of *n*-heptane/ethanol 90:10 (v:v) using a preparative HPLC system provided by Knauer (Berlin, Germany), which consisted of a K-1800 pump with a 1000 mL/min pump head, a HPLC-Box and a K-2500 UV detector. The flow rate was 50 mL/min for **H5** and **H6** and 100 mL/min for **H4**, leading to run-times of 20 min per injection. The injection volume was 3 mL of approx 40 mg sample dissolved in ethanol/heptane at various compositions. Detection was performed at 254 nm. All preparative separations were performed at room temperature (approximately 22 °C). The eluent and the HPLC column were at room temperature.

* Corresponding author. Dipartimento di Scienze Biomediche e Biotecnologie, Università di Brescia, viale Europa 11, 25123 Brescia, Italy. Telephone: +39-0303717415. Fax: +39-0303701157. e-mail: abbate@med.unibs.it.
[†] Università di Brescia.
[‡] UdR Brescia.
[§] CarboGen AG (Aarau).
[||] Università di Bergamo
[⊥] Politecnico di Milano.

10.1021/jp0456537 CCC: $27.50
Published on Web 12/04/2004

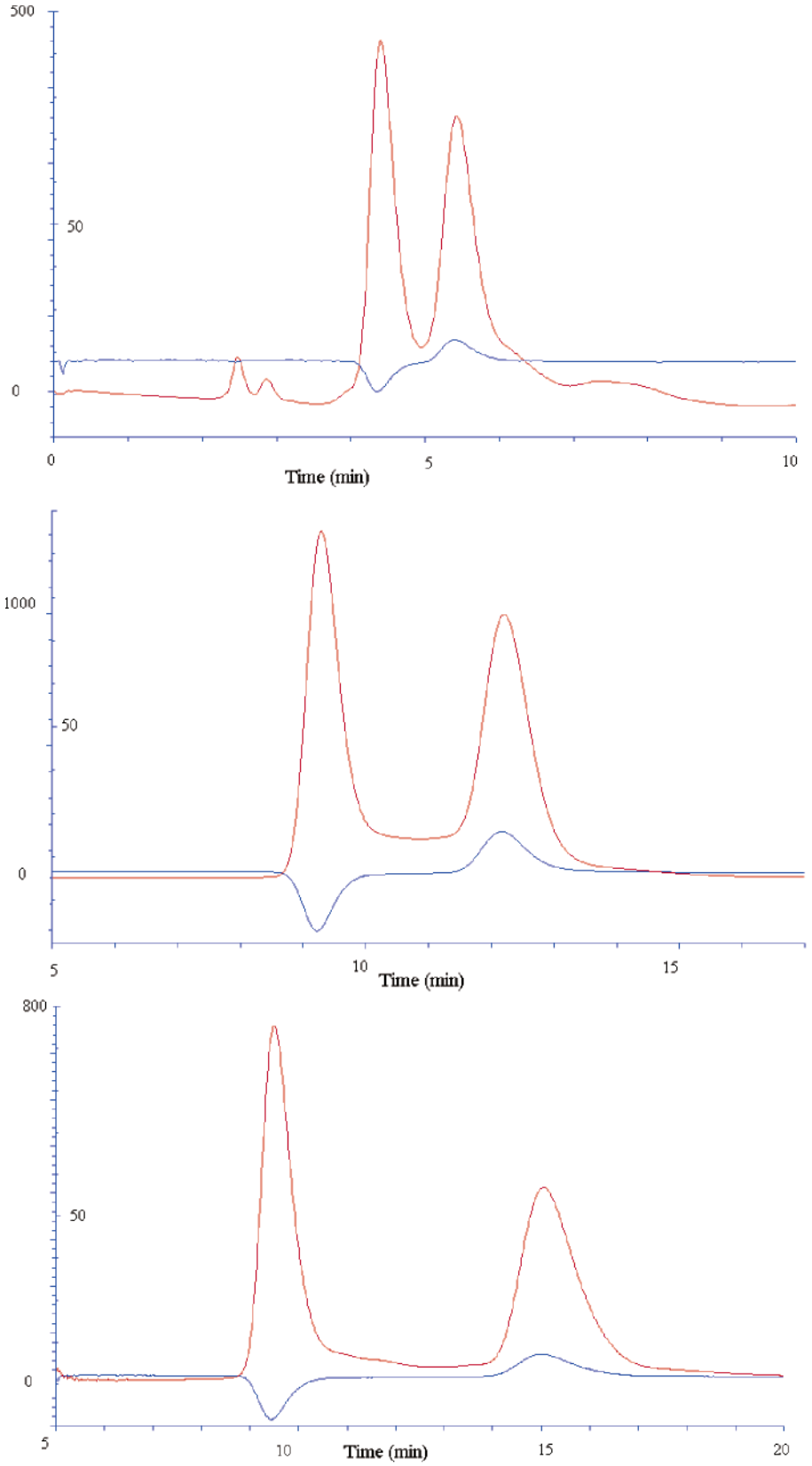

Figure 1. UV and polarimetric detection during enantioselective semipreparative HPLC on Chiralcel OD of 4-aza[5]helicene (top traces), 5-aza[5]helicene (middle traces), and 6-aza[5]helicene (bottom traces). The outer ordinate scales are in mAU (AU = absorbance units). The inner ordinate scales are in millivolts and come from the voltage output of the polarimeter. For chromatographic details see the Experimental Section.

The obtained fractions were analyzed using a HP 1090 system equipped with an analytical HPLC column (Chiralcel OD 250 × 4.6 mm, 20 μm). The sample room from the HP 1090 systems was kept under exclusion of light. The mobile phase was *n*-heptane/ethanol 90:10 (v:v) under isocratic conditions. The injection volume was 250 μL of the analyzed fraction without dilution. The run-time was 20 min at a flow rate of 1 mL/min at ambient temperature. Detection was at 254 nm. In Figure 1, the chromatograms of the three preparative separations are depicted. The red color indicates the UV-detection at 254 nm,

TABLE 1. Comparison of Observed Wavelengths (nm), and *A* and Δ*A* for 4-Monoaza[5]helicene (4), 5-Monoaza[5]helicene (5), 6-Monoaza[6]helicene (6), and [5]Helicene (A, ref 23; B, ref 8)[a]

H4				H5				H6				[5]-carbohelicene			
UV		CD		UV		CD		UV		CD		CD_A[23]		CD_B[8]	
λ (nm)	A	λ (nm)	$\Delta A \times 10^5$	λ (nm)	A	λ (nm)	$\Delta A \times 10^5$	λ (nm)	A	λ (nm)	$\Delta A \times 10^5$	λ (nm)	Δε	λ (nm)	Δε
394	0.046			396	0.044			393.6	0.003			395	vw	394	vw
374.5	0.047			375	0.047			374.6	0.003			376	+0.5		
331.5	0.125	327.6	−11	331	0.45	330	−36.6	331.8	0.021	327.2	−3.8	328	−134.7		−127
310	0.175 sh	306	−29	309 sh	0.809	305.6	−97	312.6 sh	0.032	307	−11	309	−299.1	305	−327
298	0.215	291.8	−13	296.5	0.903	289.2 sh	−22.7	297.4	0.043	291.4	−3.9				
		283	−9.5			275.2	−17.2			283.2	−3.3				
260	0.231	267.6	−4.1	263.5	0.941	263.4 ?	−8.4	259.8	0.047	267	−1.3				
253	0.209 sh	252.4	+11	255 sh	0.785	250.4	+12.7	253 sh	0.041	252.2	+4.3	272	+73.9		
		246.8	+11							247	+4.3	263	+76	268	+170
		233.4	−10			231.8	−53.2			232.6	−2.6	236	−63.8		−54
227	0.621	225.6	+10	227.5	2.35	221.6	+28	227	0.140	226	+4.7	229	+25.1		
		215	−11							217	−5.7				
												207	+212.5		+209

[a] For the latter two cases we report only CD data in Δε units (L/mol cm). The values for column B were estimated by us on the original CD spectra reported in ref 8.

TABLE 2. Comparison of Calculated Geometrical Characteristics and Racemization Barriers (Δ*E*) for 4-Monoaza[5]helicene (H4), 5-Monoaza[5]helicene (H5), 6-Monoaza[5]helicene (H6), and [5]Helicene (carbo)[a]

	H4	H4 (X)	H4 (X)	H5	H5(X)	H6	H6 (X)	carbo
C−C−C−C (center)	−29.1	30.6	−32.6	−28.4	29.8	−29.9	−27.4	−29.8
C−C−C−C (N side)	−18.0	16.1	−18.0	−16.6	15.4	−16.0	−18.6	−17.8
C−C−C−C	−18.2	18.6	−16.6	−18.2	17.6	−17.8	−17.6	−17.8
CC int	1.44	1.429	1.430	1.44	1.433	1.44	1.433	1.44
CC front	1.37	1.387	1.343	1.37	1.340	1.37	1.345	1.37
CC others	1.42	1.399	1.403	1.42	1.408	1.42	1.410	1.42
CN	1.32	1.355	1.313	1.30	1.300	1.30	1.294	
CN′	1.36	1.366	1.399	1.38	1.378	1.38	1.372	
pitch-internal C (10^{-2} Å/deg)	0.72			0.71		0.71		0.73
pitch-remaining C (10^{-2} Å /deg)	0.98			0.98		0.99		1.01
$z_2 - z_{13}$ (Å)	3.35			3.30		3.34		3.40
Δ*E* (kcal/mol)	23.2			22.2		22.9		24.1[b]

[a] Dihedral angles (CCCC) are in degrees. CC int is the average C−C bond length for the inner carbons, CC front for C−C bond in front of them (see text and structures). The helical pitch is defined in the text. The barrier height (Δ*E*) is in kcal/mol. [b] Other calculations give 22.7 kcal/mol,[20] 25.5 kcal/mol.[21]

while the blue color indicates the online polarimetric detection at 653 nm.

(b) CD and UV Spectra. After chromatographic separation, the enantiomer fractions were evaporated using a rotavapor at a water-bath temperature of 5 °C, at a reduced pressure of 40 mbar. The dried samples of enanatiomerically enriched helicenes from chromatography were stored at −20 °C under N_2 before use. For the CD experiments, the same protocol was followed for all samples: the collected fraction was dissolved in methanol, that had been previously stored at −4 °C, and the CD spectra were immediately recorded using a 0.1 cm quartz cuvette. The cuvette, initially at −4 °C, was allowed to warm to room temperature during the course of successive measurements. Spectra were taken on a JASCO 500 spectropolarimeter flushed with dry nitrogen at room temperature. After racemic equilibration had been reached, UV spectra were recorded on a Jasco 800 UV−vis spectrophotometer using the same filled cuvettes from the CD experiments.

In Figure 2, we report the UV and CD spectra of **H4**, **H5**, and **H6**. CD spectra were recorded every 2.5 min, with the first taken just after dissolving the solid sample in −4 °C methanol. To have less congested figures we report only four traces for each enantiomer (see figure caption). A summary of the main characteristics of the CD and absorption spectra of the three molecules is given in Table 1. There we do not report the values for the molar extinction coefficients ε and Δε, since we do not know the enantiomeric excess of the sample (see section IVa).

III. Calculations

Ab initio calculations were performed employing the GAUSSIAN-98 package[16] to determine the optimized geometry of the equilibrium-conformations of each enantiomeric pair and the enantio-inversion transition state (TS) conformation of [5]helicene, of **H4**, **H5**, and **H6**. The DFT method was adopted, taking the B3LYP functional[17,18] and 6-31g** basis functions.[19] The TS geometry for each molecule was determined by the method of quadratic synchronous transit QST of the Gaussian package, developed therein on the basis of ref 19: once given the optimized geometries of the two minima, the first-order saddle point is searched and optimized. We report in Table 2 the energy barrier to racemization (Δ*E*) and some geometric parameters, that were evaluated on the basis of the calculated geometries of the minima; the latter data are compared with the corresponding data from X-ray structures of ref 15, and will be commented on later. For **H4**, we show in Figure 3 the vibrational displacements for the lowest frequency normal mode of the equilibrium geometry as well as for the imaginary frequency mode found at the TS: the displacements are suggestive of the transition pathway. Quite similar results are obtained for **H5** and **H6**. All these results are also quite similar to those found for carbohelicenes in previous ab initio calculations.[9,20,21]

The hypothesis of racemization via a nonbond-breaking conformational path and exclusion of a bond-breaking path or formation of a Diels−Alder adduct has already been discussed

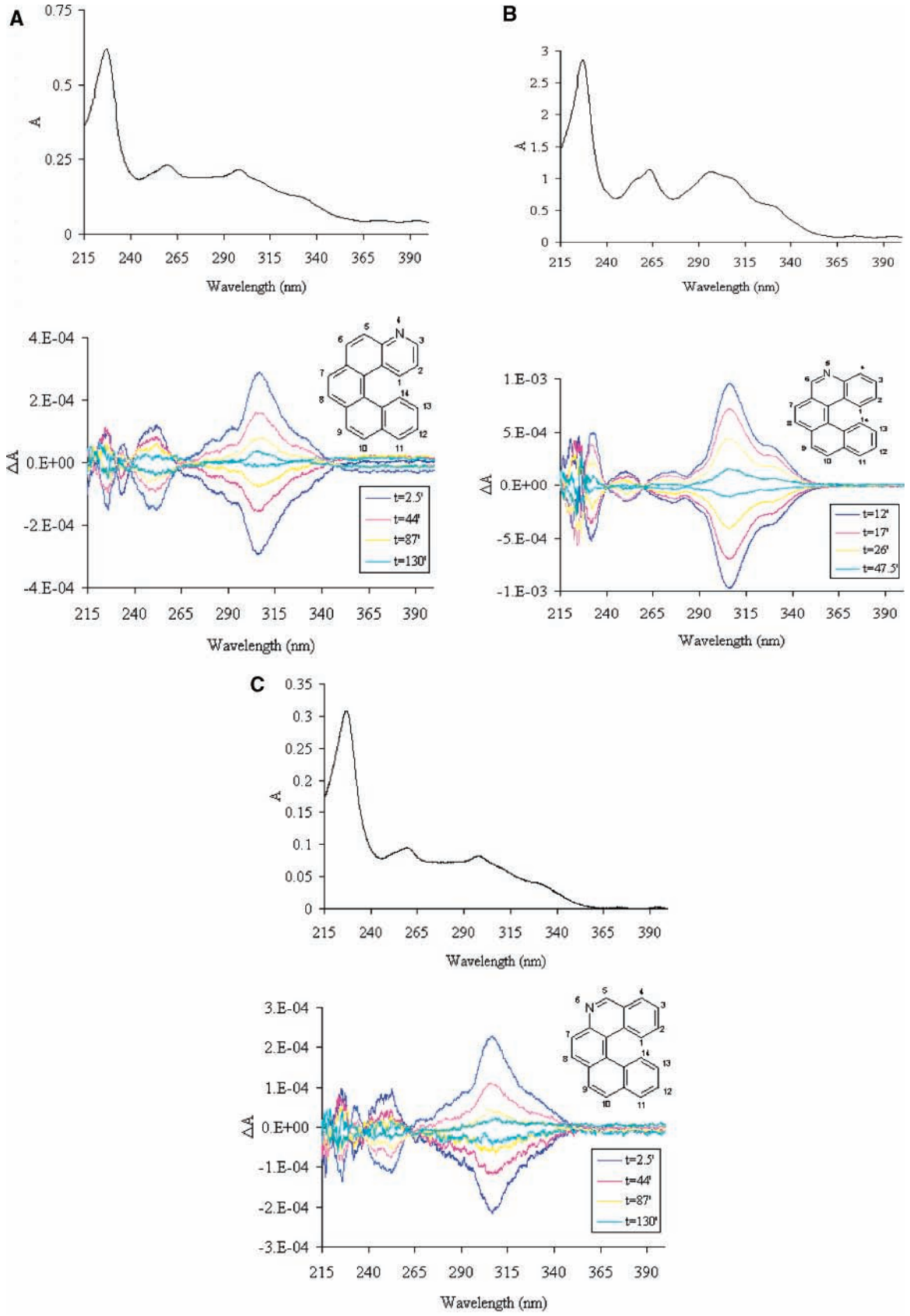

Figure 2. UV and CD spectra of both enantiomers of **4**-aza[5]helicene (**H4**) (A), **5**-aza[5]helicene (**H5**) (B), and **6**-aza[5]helicene (**H6**) (C). Spectra were recorded in the same 1 mm quartz cell under identical conditions (see text). Four CD spectra from each enantiomer are given at four different racemization times (see text). The CD spectra with the positive band at ca. 306 nm in all three azahelicenes are for the enantiomer which was eluted second (positive OR).

for the cases of carbohelicenes in refs 2, 22, and 23. We hope to provide here further convincing evidence of that mechanism.

TDDFT calculations have been carried out on the same optimized geometries, with the updated version of Gaussian package, Gaussian-03.[24]

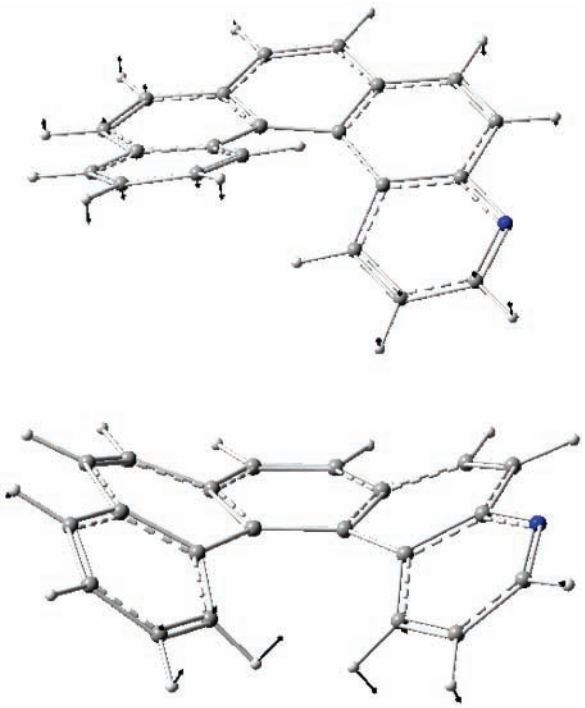

Figure 3. Equilibrium (top) and transition state (bottom) conformations of **4**-aza[5]helicene (**H4**), as calculated ab initio on the basis of GAUSSIAN 98 package.[16] Lower frequency displacements for equilibrium geometry and displacements associated with the imaginary frequency for TS are reported, as shown by Gaussview.[16]

IV. Results and Discussion

(a) Enantioselective Chromatography and Racemization under Chromatographic Conditions. Preparative enantiomer separation was performed as described in the Experimental Section. It should be noted that not all samples were chemically pure. Looking at Figure 1, one may notice that all three azahelicene enantiomers with the negative sign of optical rotation (which can be attributed to the **M** enantiomers,[26] as we have observed for other heterohelicenes[13]) elute first. The shape of the chromatograms indicates that the enantiomerization of separated species already takes place during chromatography. This effect is especially pronounced for **H5**, where the raised baseline between the two enantiomers indicates racemization during chromatography. Therefore, the isolation of compounds with an ee > 87%, as determined by analytical methods, was not possible. For this reason we were not able to determine the specific rotation of the samples; however we point out that in Figure 1 relative values of the optical rotation for the three helicenes can be evaluated.

(b) Assignment of the CD Spectra. As one may see from Figure 2, the CD signals for **H4**, **H5**, and **H6** indicate a ready racemization that has been observed in general for smaller helicenes at room temperature.[20,23]

The UV and CD spectra of **H4**, **H5**, and **H6** are quite reminiscent of the UV and CD spectra of the "parent" molecule [5]helicene.[25] On the basis of this comparison, we assign the **M** configuration[26] to the enantiomers of **H4**, **H5**, and **H6** showing a negative CD band centered at ~306 nm and the **P** configuration to the enantiomers showing a positive band there. It is indeed recognized that the electronic transition corresponding to such CD band determines the minus (plus) sign for the rotation at the sodium D line for the **M** (**P**) enantiomer. This is also consonant with the results of Figure 1 of the present work.

However, the CD spectra of the three monoazahelicenes are not exactly identical to the CD spectra of [5]helicene (see Table 1). We notice that the most intense CD band centered at ~309 nm for [5]helicene[23] corresponds to the bands observed at ~306 nm for **H4**, **H5**, and **H6**. Moreover, structured features appear at ~267, 283, and 291 nm for **H4** and **H6** without any correspondence with [5]helicene.[8,23] This structuring does not have the same appearance in **H5**. Indeed as seen in Figure 2B, the CD spectrum of **H5** presents a negative shoulder at ~289 and a broad negative dissymmetric band at ~275 and 263 nm. In all these cases, the difference between two consecutive features is in the range of 2000 and 1000 cm^{-1}. Whether these sub bands are of vibronic origin needs future investigation. **H5** exhibits also an evident sideband at ~330 nm, that is just a minor shoulder for **H4** and **H6**.

In the central part of the spectrum, the features at 272 and 263 nm, observed for [5]helicene,[8,20] are shifted for **H4**, **H5**, and **H6** toward lower wavelength (~250 nm, see Table 1).

At low wavelength the major difference between [5]helicene and compounds **H4**, **H5**, and **H6** is that the weak negative CD signal observed at ~236 nm for [5]helicene[8,20] is still shifted toward lower wavelength for the aza[5]helicenes (see Table 1). We observe also a band at ~226 nm that could correspond to the shoulder reported at 229 nm for [5]helicene.[8,20]

These CD spectra will be compared with the results of ab initio TD-DFT calculations in part e of this section.

(c) Kinetics of Racemization. From the CD spectra that were taken each 2.5 min, we were able to determine that the kinetics of racemization for **H4**, **H5**, and **H6** is a first-order process. Kinetic constants (k) and half-life times ($t_{1/2}$) were determined by plotting the logarithm of the ellipticity of the most intense CD band vs time. The plot is typical of first-order process (see Figure 4) and the slope corresponds to the kinetic constant k and further $t_{1/2} = (\ln 2)/k$. The kinetic measurements were repeated twice for each enantiomer of **H6** and were performed once for **H4** and **H5**. The results of Figure 4 give well-defined values for the rate constants k for both enantiomers of each azahelicene under study. Differences between the k values of enantiomeric pairs are irrelevant for **H5** and **H6**; the noncoincidence observed for **H4**, where the k values are smaller, is probably due to the noncontrol of constant temperature in the present study. We finally propose to take for the k values the averages of each enantiomeric pair reported in Figure 4: $k = 0.015\ min^{-1} \pm 0.002$ and $t_{1/2} = 47\ min \pm 5$ for **H4**, $k = 0.061\ min^{-1} \pm 0.002$ and $t_{1/2} = 12\ min \pm 1$ for **H5**, and $k = 0.020\ min^{-1} \pm 0.001$ and $t_{1/2} = 35\ min \pm 1$ for **H6**.

In the literature,[2,23] [5]helicene is reported to have $t_{1/2} = 62.7$ min at 57 °C. Since our data are recorded at room temperature, *we conclude that for the azahelicenes **H4**, **H5**, and **H6**, racemization proceeds much faster than for [5]helicene*. A more accurate kinetic study for the determination of activation energies with CD measurements taken at different temperatures will be conducted as soon as more sample will be available to us.

(d) Ab Initio Calculations: Ground-State Characterization. One motivation of ab initio calculations has been to find a rationale for the different behavior in the racemization rate of **H4**, **H5**, **H6**, and [5]helicene. At first sight, it is pleasing to notice that the calculated barriers (see Table 2) correlate with what experimentally observed, i.e. $t_{1/2}$(**H4**) > $t_{1/2}$(**H6**) ≫ $t_{1/2}$(**H5**). As indicated in ref 20, the results may be largely influenced by different functional and (especially) basis function choices. For this reason we decided to run a calculation of our own for [5]helicene with exactly the same method to locate transition state as for **H4**, **H5**, and **H6**. For [5]helicene we obtain an intermediate value between those reported in the literature:

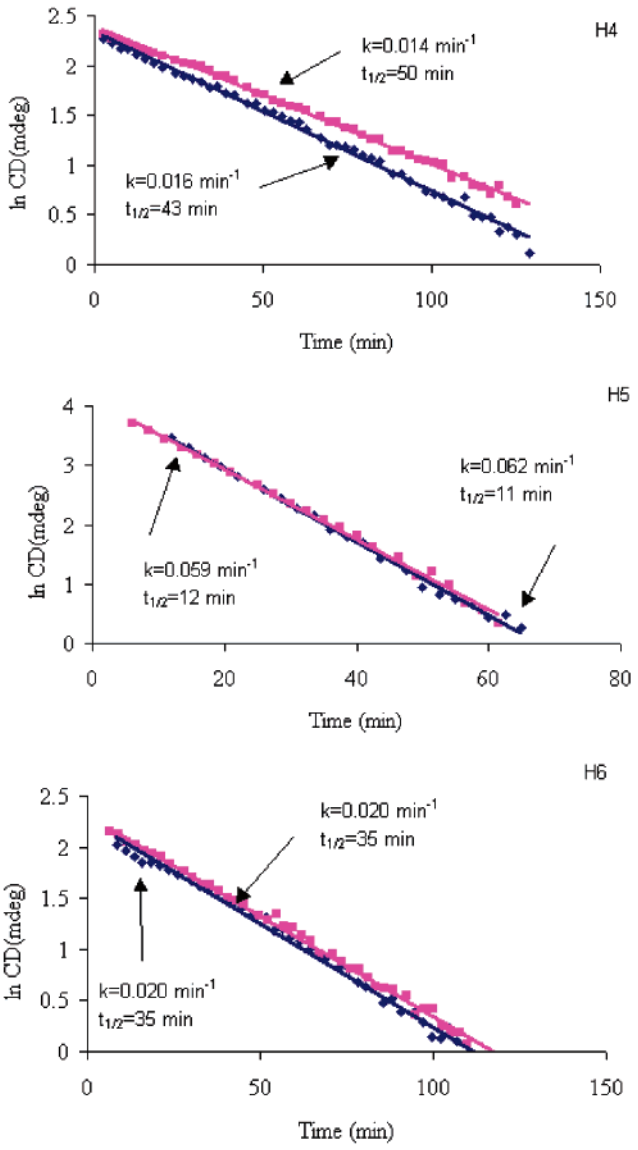

Figure 4. Logarithm of the ellipticity θ of the major CD bands at ca. 306 nm vs time for **4**-aza[5]helicene (**H4**, top), **5**-aza[5]helicene (**H5**, center), and **6**-aza[5]helicene (**H6**, bottom). The slope corresponds to the kinetic constant and $t_{1/2} = (\ln 2)/k$ for a first-order process. For **H4**, **H5**, and **H6** the trace of each enantiomer is reported on the figure.

22.7 kcal/mol in ref 20 and 25.65 kcal/mol in ref 21; the value found by us suggests a slightly slower racemization for this compound, as indeed observed in refs 2 and 23. From Table 2 one notices that geometries are very similar in all four molecules, and also the barriers are similar.

Considering the lower frequency vibration for the equilibrium geometries, and the displacements associated with the imaginary frequency calculated at the saddle point (Figure 3), we can describe the reaction coordinate. The vibration is practically the same for **H4**, **H5**, **H6**, and [5]helicene; namely it is an antisymmetric out-of-plane bending for the most external H atoms in the terminal phenyl rings. The same transition structure and the same type of vibration has been described for carbohelicenes in recent studies.[20,21]

From the above kinetic data it can be concluded that racemization for **H4**, **H5**, and **H6** is a unimolecular reaction with a rate constant $k_i = A_i \exp(-E_i^*/kT)$, (i = **H4**, **H5**, **H6**), where E_i^* are the energies of the transition structures for the three molecules.[27] Since the transition structures of the three molecules are almost the same, one may assume that the preexponential factor A_i is the same for the three molecules. In this way we find $k_{\mathbf{H4}}/k_{\mathbf{H5}} = \exp((E_{\mathbf{H5}}^* - E_{\mathbf{H4}}^*)/kT = 0.19$ at room temperature ($T = 298$ K), to be compared with the experimental value of 0.25. We also find $k_{\mathbf{H6}}/k_{\mathbf{H5}} = 0.31$, to be compared with 0.33. This excellent agreement between theory and experiment lends support to DFT calculations, as well as to the proposed mechanism of racemization.[2]

Finally, the equilibrium geometry is quite similar in all four molecules: the five internal C−C bonds, especially the three central ones (denoted a−b, b−c, and c−d in the structures within the text), are longer than the others and have partial single-bond character; the C−C bonds in front of them (5−6, 7−8, and 9−10; indicated in the table as C−C front) are the shortest ones and have double-bond character. We have calculated the helix pitch adopting a Cartesian system centered in the point determined by the average position of all carbon and nitrogen atoms, with an *X*-axis intersecting the middle point between carbon atoms 7 and 8 (see structures) and being the *Y*-axis parallel to the C−C bond joining these two atoms. As in ref 20, the pitch (**p**) is such that for each heavy atom i, $z_i = \mathbf{p}\varphi_i$ being $\varphi_i = \arcsin [y_i/(x_i^2 + y_i^2)^{1/2}]$. The helix is less extended for the inner carbon atoms than for all the others, for this reason we give two different values for the pitch. In any case they result in the same values for all four molecules. A slight difference among geometries is better evidenced just considering the end to end helix *Z*-distance, i.e., the difference between *Z*-coordinates of carbons 2 and 13 (reported in Table 2) or between carbons 1 and 14. The trend of these quantities follows the energy barriers; in particular for $Z_2 - Z_{13}$ there is a nice linear dependence on ΔE (see Table 2).

(e) Ab Initio Calculations: CD Spectra. Using the updated version 2003 of the GAUSSIAN package[24] and the TD-DFT method with the 6-31G(d,p) basis set, we also calculated the CD spectra of the three molecules that we examined experimentally, plus [5]helicene. The TD-DFT method has already been used in the literature for the study of helicenes and turned out to be a valuable tool for the interpretation of CD spectra.[10] In the present context, the aim of CD calculations is mainly a qualitative interpretation of the experimental spectra. Technical issues, such as the dependence of results on the basis set and on the DFT functional, or comparisons with other methods, are not discussed here. However, for more accurate predictions, as we plan to do in future works, an investigation of such issues will be necessary, in view of the known critical aspects of the various available methods for CD calculations, as pointed out for example in ref 28.

The first 25 excitations in order of increasing energy have been taken into account, and the corresponding rotational strengths have been calculated. The **P** helicity configuration, corresponding to positive optical rotation,[2,5] has been used in all the calculations presented below. The calculated values of rotational strengths in esu^2 cm^2 (cgs units) $\times 10^{40}$ and the calculated values of the corresponding wavelengths in nanometers are given in Table 3. The calculated CD spectra of **H4**, **H5**, and **H6**, simulated by Gaussian band shapes[29] (in black), are shown with the experimental spectra (in red) for sake of comparison, in Figure 5a, where the bars are proportional to the calculated rotational strengths. For completeness we also report the calculated spectrum of carbohelicene.

The most noticeable aspect of these results is the presence of a large rotational strength feature in the region 314−318 nm, found in the four different helicenes, that may be identified with the main positive band that characterizes the experimental data,

TABLE 3. Comparison of Calculated Wavelengths λ, and Rotational Strengths R for [5]Helicene, 4-Monoaza[5]helicene (H4), 5-Monoaza[5]helicene (H5), and 6-Monoaza[5]helicene (H6) Where Rotational Strengths Are in esu^2 cm^2 $\times$ 10^{40}

[5]helicene		H4		H5		H6	
λ (nm)	$10^{40}R$ (cgs)	λ (nm)	$10^{40}R$ (cgs)	λ (nm)	$10^{40}R$ (cgs)	λ (nm)	$10^{40}R$ (cgs)
364.3	−1.9	365.1	14.4	361.2	−1.8	361.6	−1.6
341.0	−1.9	341.0	−0.9	339.8	−2.0	342.0	−2.5
316.1	376.4	318.0	258.4	314.0	345.8	317.6	293.2
305.8	−99.6	309.6	−70.0	308.0	−53.4	313.9	−55.6
301.5	2.3	296.9	−12.5	301.1	21.0	293.3	−30.2
293.8	−4.1	290.1	97.6	296.0	−91.1	290.5	−24.7
278.3	−46.6	283.1	−61.7	293.5	17.9	289.4	37.4
269.8	3.2	278.9	−34.2	274.4	−0.5	279.3	8.6
263.1	0.9	270.1	−10.1	268.7	−4.4	270.6	0.3
258.0	−11.9	266.5	9.2	267.6	−4.0	269.9	−24.0
244.9	7.6	261.1	−1.1	265.6	2.0	257.0	−39.0
235.0	0.0	257.2	−7.0	256.1	−19.2	253.0	17.4
232.6	291.5	245.0	1.9	241.2	9.2	243.8	16.1
230.1	25.3	237.1	40.5	234.5	122.9	235.0	52.5
227.1	1.2	233.0	91.2	234.2	42.8	232.1	97.2
220.9	−114.6	232.4	67.2	232.1	8.2	231.9	−3.8
217.9	0.2	227.1	15.1	226.8	84.1	230.1	123.8
216.3	12.2	223.4	5.1	224.0	61.0	223.1	−13.3
215.7	−66.4	219.9	−6.9	220.4	−40.5	219.3	−94.0
215.1	14.9	216.9	3.3	219.1	−68.1	218.5	17.1
209.9	−73.2	215.6	63.6	215.1	−35.0	215.9	14.5
205.3	8.8	214.2	2.3	213.4	1.6	215.1	−66.1
203.1	8.4	211.7	−92.9	210.7	6.9	212.3	−1.4
202.5	−1.6	210.6	−16.6	208.5	−7.0	208.9	−23.2
198.9	7.8	207.8	−20.2	205.7	−115.0	206.7	−17.8

both for [5]helicene, as already reported in the literature,[8] and for the **H4**, **H5**, and **H6** molecules in this work. The wavelength of this band is calculated ca.10 nm above the experimental result for the peak of the main positive band. Overall, the calculations do not display important differences for this wavelength among the four molecules under consideration. The presence of structured features on the left side of this band, observed both in **H4** and in **H6**, might correspond to the calculated positive CD feature at 290.1 nm in **H4**, and 289.4 nm in **H6**. On the other hand, if one looks at experimental data, the positive left-hand side of the 308 nm peak decreases more steeply in the parent molecule, [5]helicene,[8] and has a definitely different shape in **H5**. Pleasing correspondence with the calculations is found, in that no significant feature is calculated for the [5]helicene molecule and an important negative feature is calculated for **H5** at 296.0 nm (see Table 3 and Figure 5a).

No appreciable positive feature is calculated on the right side of the major CD band of all four helicenes under theoretical investigation; in the main, two minor negative transitions are calculated some distance removed. Thus, no clear interpretation of the observed positive shoulder of all four helicenes can be provided.

Also an interpretation of the experimental negative broad feature between 270 and 230 nm is somewhat difficult to make on the basis of the present calculations. However, we observe that a negative intense CD feature is predicted for **H6** at 257.0 nm; the same negative band is calculated at 258 nm in carbohelicene and is much less intense there. For **H4** and **H5** we calculate less intense CD lines at 257.2 and 256.1 nm. This is consistent with the observation made above in section IVb that the negative CD band is shifted toward lower wavelengths upon substitution of a CH group with a nitrogen atom.

The observed positive peak at ca. 233 nm can be thought to correspond to one or several calculated positive features between 240 and 225 nm. Also, the next negative CD band observed at ca. 225 nm correlates with a calculated negative transition at either 219 or 220 nm, and, in this sense, better correspondence is found for **H5** and **H6**.

As a final comment, we note that the TD-DFT calculations presented above are in fair correspondence with the experimental CD spectra. This can be further appreciated if we choose to represent our calculated results by assigning a Gaussian profile to each calculated line.[29] Assuming the same approach for representing calculated CD curves as in the work by Mason et al.,[8] a bandwidth of $\sigma_\nu = 7.5\nu^{1/2}$ (with σ_ν and ν in cm^{-1}) is adopted for the frequency spectrum; the corresponding width in wavelength is given by the relationship $\sigma_\lambda = 7.5\lambda^{3/2}$ (with σ_λ and λ in cm) that amounts to $\sigma_\lambda = 7.5$ nm at $\lambda = 215$ nm and $\sigma_\lambda = 16.5$ nm at $\lambda = 365$ nm. The results are reported in Figure 5a for the CD spectra and in Figure 5b for the absorption spectra. The results clearly indicate where the most pronounced effects from the N atom are found between 280 and 225 nm in the spectra. This has been shown also in some preliminary results for naphthalene and phthalazine.[30] Let us now turn to a critical analysis of the theoretical results.

According to the configuration-interaction (CI) approach exploited in the GAUSSIAN package, single-electron transitions between several molecular orbitals are involved in the determination of each transition (see the Supporting Information for the details).

For the sake of understanding, normalized transition electric dipole moments $\vec{\mu}/|\vec{\mu}|$ (with $\vec{\mu} = \langle 0|\hat{\vec{\mu}}|b\rangle$) and magnetic dipole moments $\vec{m}/|\vec{m}|$ (with $\vec{m} = \langle 0|\hat{\vec{m}}|b\rangle$) are reported in Table 4 for the different helicenes and for some selected excited states. The purpose of this table is to illustrate the orientation and symmetry

TABLE 4. Normalized Transition Electric ($\vec{\mu}/|\vec{\mu}|$) and Magnetic ($\vec{m}/|\vec{m}|$) Dipole Moments of Some Spectral Lines for [5]Helicene (Carbo), 4-Monoaza[5]helicene (H4), 5-Monoaza[5]helicene (H5) and 6-Monoaza[5]helicene (H6)[a]

	λ (nm)	$10^{40}R$ (cgs)	$\mu X/\|\mu\|$	$\mu Y/\|\mu\|$	$\mu Z/\|\mu\|$	polarization assignment	$mX/\|m\|$	$mY/\|m\|$	$mZ/\|m\|$	type
carbo	316.1	376.4	0.99	0	−0.16	b	−0.09	0	1.00	t
	293.8	−4.1	0	1.00	0	a	0	1.00	0.01	r
	258.0	−11.9	0	1.00	0	a	0	1.00	0	r
H4	318.0	258.4	0.03	0.43	0.90	n.d.	0.04	−1.00	−0.05	r
	290.1	97.6	−0.23	−0.47	−0.85	n.d.	0.68	0.49	0.55	r, t
	257.2	−7.0	−0.96	0.13	−0.24	b	−0.30	−0.95	0.10	r
H5	314.0	345.8	0.09	0.43	0.90	n.d.	0.10	−0.99	−0.07	r
	293.5	17.9	0.34	0.46	0.82	n.d.	−0.99	0.08	−0.07	*r*,t
	256.1	−19.2	−0.93	−0.03	−0.38	b	−0.92	−0.28	0.27	t
H6	317.6	293.2	0.01	−0.44	−0.90	n.d.	0.02	1.00	0.07	r
	289.4	37.4	0.64	0.37	0.67	∼b	0.13	−0.97	−0.18	r
	257.0	−39.0	0.93	−0.24	−0.28	∼b	0.63	−0.78	−0.08	r

[a] Rotational strengths are in 10^{40} esu^2 cm^2. "a" and "b" are symmetry or pseudo-symmetry labels (see text). "t" and "r" are used to design tangential and radial transitions respectively (see text).

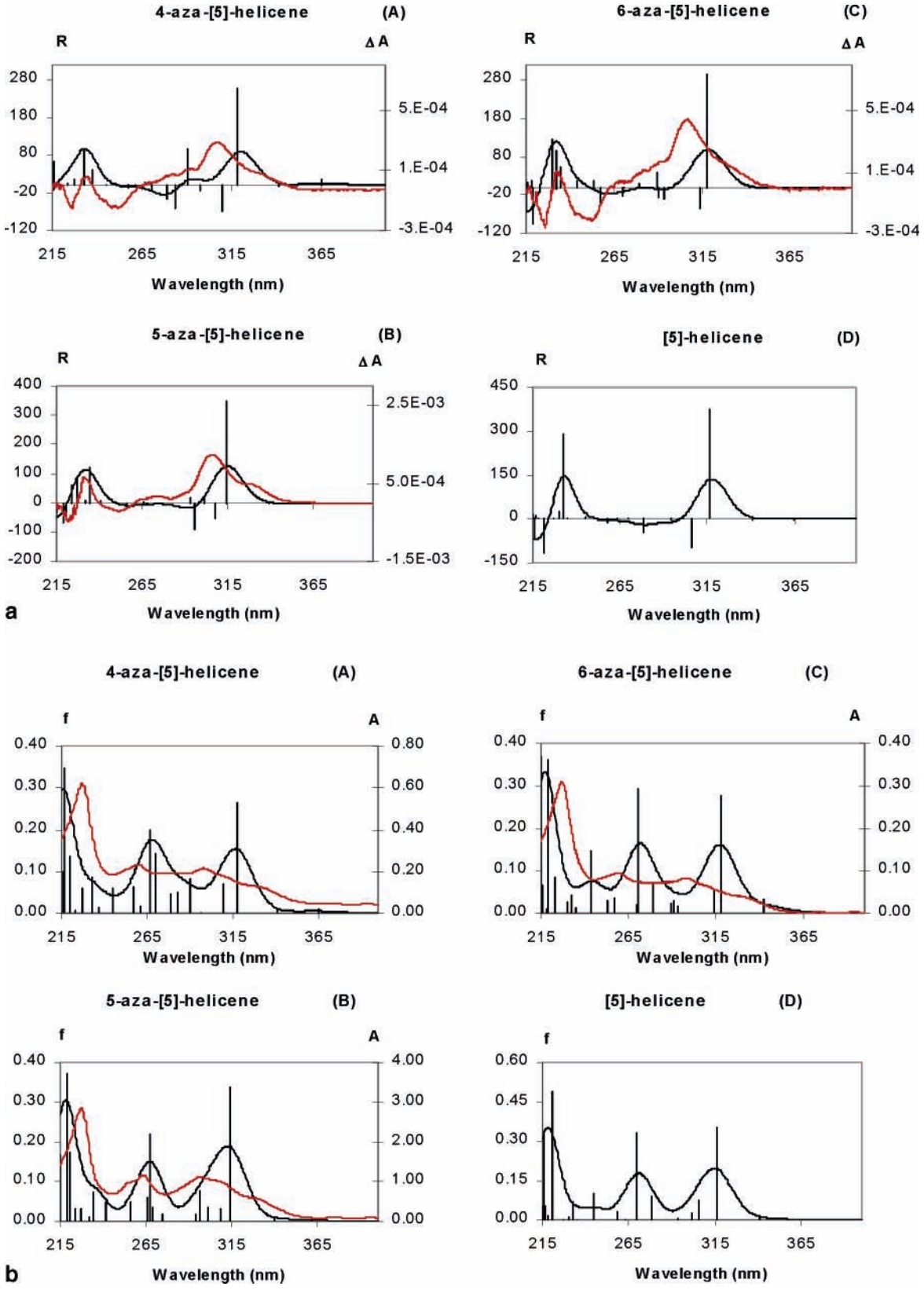

Figure 5. (a) Calculated CD spectra for the **P** forms of **4**-aza[5]helicene (**H4**, A), **5**-aza[5]helicene (**H5**, B), **6**-aza[5]helicene (**H6**, C), and [5]helicene (**carbo**, D). The calculations are given as bars, the heights of which are equal to the calculated rotational strengths in esu^2 cm^2 $\times$ 10^{40} (see Table 3). Calculated Gaussian band shapes are shown as black curves that are superimposed on the corresponding experimental CD spectra, reported as red curves, for the three monoazahelicenes (values of ΔA shown on the right axis). (b) Calculated absorption spectra for the P forms of **4**-aza[5]helicene (**H4**, A), **5**-aza[5]helicene (**H5**, B), **6**-aza[5]helicene (**H6**, C) and [5]helicene (**carbo**, D). The calculated oscillator strengths (f) are given as bars and are also assigned a Gaussian profile (see the text), as represented by the black curves. The experimental absorption spectra are represented as red curves (values of A shown on the right axis).

of transition dipole moments. The values of the vector components represent a more detailed analysis with respect to the rotational strengths: as a consequence, they can be expected to be in general more delicate and more sensitive to the choice of

the basis set. As stated above, a thorough analysis of the basis dependence of results is beyond the scope of this work. However, some preliminary calculations, for the case of **H4**, with two different basis sets (namely 6-311++G** and TZVP of Gaussian03) give results in very good agreement with the data reported in Table 4, so that the qualitative properties discussed below seem to be independent of the basis choice. The vector components are given with respect to a reference frame, where the *Y*-axis is parallel to the C_2 symmetry axis of the parent molecule [5]helicene, the *Z*-axis is parallel to the helix axis, and the third axis, *X*, forms a right-handed Cartesian coordinate system with *Y* and *Z*. The same coordinate system is maintained for the azahelicenes. The polarization assignments in this table refer to the standard notation that uses letters "a" and "b" to designate parallel and orthogonal polarization to the C_2 symmetry axis, respectively.[31] This assignment is very clear in the case of carbo[5]helicene, where the polarization unit vectors are exactly parallel or orthogonal to the *Y*-axis, reflecting the real symmetry of the molecule, and indicating in particular that the main positive CD band (at 316 nm in the calculation) has a "b" polarization and thus corresponds to a state belonging to the B irreducible representation of the symmetry point group C_2, in agreement with previous studies in the literature.[8−10]

On the other hand, the polarization in azahelicenes is very different and in general cannot be defined as parallel or orthogonal to the *Y*-axis. Of course, the absence of a definite "a" or "b" character of the excited states is a consequence of the lack of symmetry due to the substituent nitrogen atom; however, an assignment is given in Table 4, with a rough estimate of the degree of symmetry, where the following convention has been adopted: the line is defined as "b" if the absolute value of the Y component is less than 0.2 and "∼b" if it is between 0.2 and 0.4; the same criterion is applied to the component orthogonal to the *Y*-axis, with the letter "a" instead of "b". For those cases that do not match any of these conditions, the notation "n.d." (not defined) is used. The magnetic dipole moments shown in the last three columns of Table 4, if compared to electric dipole moments, are more easily identified as parallel or orthogonal to the helicene symmetry axis (*Y*-axis in our case), but they show remarkable changes from one species to another.

Concerning the main positive CD band, it can be observed that μ has approximately the same polarization direction in **H4**, **H5**, and **H6**, with the main component along the *Z*-axis, but with a significant component along the *Y*-axis. This prevents one from assigning a definite polarization according to the conventions used above and is in contrast to the [5]helicene, where the polarization of this band is along the *X*-axis; a similar behavior is found in the case of magnetic dipole moments, that are along the *Y*-axis in the aza[5]helicenes and along the *Z*-axis in [5]helicene.

In the region at 256−258 nm, the electric dipole moments of **H4, H5**, and **H6** are still almost parallel to each other. In this case the μ polarization of azahelicenes is approximately "b" while the [5]helicene has "a" polarization. Following ref 9, we may say that for [5]helicene "b" transitions are tangential and "a" transitions are radial. This is tantamount to indicating for the former transitions charge circulation from one end of the molecule to the other (clearly in relation with the high Z-polarization of the magnetic moment), and for the latter transitions one observes high Y-components of the magnetic and electric dipole moments. Among the three lines under consideration in Table 4, in carbohelicene there are one tangential and two radial type transitions, while almost all the transitions are radial for the three azahelicenes (see the last column of Table 4). The change in character from tangential to radial is particularly evident in the first transition at ∼316 nm: this fact indicates that the overall circulation of charge needed in tangential transitions is interrupted or highly perturbed by the presence of the N atom. The two halves of the molecule contribute then to a different extent to the transitions.

IV. Summary and Conclusions

In this paper, we report on the successful separation by HPLC methods of the enantiomers of 4-, 5-, and 6-monoazahelicenes (**H4**, **H5**, and **H6**), on the subsequent CD measurements and on theoretical investigations of the ground-state properties and CD and absorption spectra thereof. **H5** is found to racemize more readily than the other two monoazahelicenes, as observed both by chromatography and by CD measurements. This is in qualitative and quantitative agreement with the ab initio DFT characterization of the transition state.

The CD spectra of the molecules examined here correlate with the corresponding data from the parent molecule, [5]helicene. Yet, interesting and characteristic differences are found, especially, in the central portion of the spectra, i.e. between 290 and 240 nm. TD-DFT calculations have allowed us to follow theoretically the experimental CD spectrum: the agreement between experiment and calculation is acceptable, but far from being perfect. However, the calculations allow one to understand the nature of the transitions beneath a given CD band. The presence of N atoms in the conjugated helix prevents the buildup of circulating-type charge movements in the electronic transitions, and this leads to a change in polarization of electric and magnetic dipole transition moments for the various transitions.

Acknowledgment. Financial support from MIUR (Ministero Italiano dell'Università e della Ricerca) is gratefully acknowledged. We thank Professors Aage Hansen, Copenhagen, Denmark, and David A. Lightner, University of Nevada—Reno, for reading the manuscript and making helpful suggestions. We dedicate this work to Professor Volker Schurig, University of Tübingen, who has been awarded the Chirality Medal for the year 2004.

Supporting Information Available: Table 1S, containing the single-electron transitions involved in some selected spectral lines, and text giving the associated discussion. This material is available free of charge via the Internet at http://pubs.acs.org.

References and Notes

(1) Newman, M. S.; Lednicer, D. *J. Am. Chem. Soc.* **1956**, *78*, 4765−4770.

(2) Martin, R. H. *Angew. Chem., Int. Ed.* **1974**, *13*, 649−660.

(3) Groen, M. B.; Wynberg, H. *J. Am. Chem. Soc.* **1970**, *92*, 6664−6665.

(4) Moradpour, A.; Nicoud, J. F.; Balavoine, G.; Tsoucaris, G.; Kagan, H. B. *J. Am. Chem. Soc.* **1971**, *93*, 2353−2360.

(5) Lightner, D. A.; Hefelfinger, D. T.; Powers, T. W.; Frank, G. W.; Trueblood, K. N. *J. Am. Chem. Soc.* **1972**, *94*, 3492−3497.

(6) Groen, M. B.; Wynberg, H. *J. Am. Chem. Soc.* **1971**, *93*, 2968−2974.

(7) Moscowitz, A. J. Ph.D. Thesis Harvard University. Cambridge, MA, 1957. Subsequently (ref 5) it was shown that this theoretical treatment predicted the wrong absolute configuration. However, this was explained (ref 5, personal communication from A.J.M.) in terms of an insufficient number of excited states in the configuration interaction.

(8) Brown, A.; Kemp, C. M.; Mason, S. F. *J. Chem. Soc. A, Inorg. Phys. Theor.* **1971**, 751−755.

(9) Buss, V.; Kolster, K. *Chem. Phys.* **1996**, *203*, 309−316.

(10) Furche, F.; Ahlrichs, R.; Wachsmann, C.; Weber, E.; Sobank, A.; Vogale, F.; Grimme, S. *J. Am. Chem. Soc.* **2000**, *122*, 1717−1724.
(11) Hansen, A. E.; Bak, K. L. *Enantiomer* **1999**, *4*, 455−476.
(12) Beljonne, D.; Shuai, Z.; Brédas, J. L.; Kauranen, M.; Verbiest, T.; Persoons, A. *J. Chem. Phys.* **1998**, *108*, 1301−1304.
(13) Caronna, T.; Sinisi, R.; Catellani, M.; Luzzati, S.; Abbate, S.; Longhi, G. *Synth. Met.* **2001**, *119*, 79−80.
(14) Moscowitz, A. *Adv. Chem. Phys.* **1962**, *4*, 67−112.
(15) Caronna, T. et al. Manuscript submitted for publication, 2004. CCDC-232489−232491 contains the supplementary crystallographic data for this paper. These data can be obtained free of charge via www.ccdc-.cam.ac.uk/conts/retrieving.html.
(16) Frisch, M. J.; Trucks, G. W.; Schegek, H. B.; Scuseria, G. E.; Robb, M. A.; Cheeseman, J. R.; Zakrzewski, V. G.; Montgomery, J. A., Jr.; Stratmann, R. E.; Burant, J. C.; Dapprich, S.; Millam, J. M.; Daniels, A. D.; Kudin, K. N.; Strain, M. C.; Farkas, O.; Tomasi, J.; Barone, V.; Cossi, M.; Cammi, R.; Mennucci, B.; Pomelli, C.; Adamo, C.; Clifford, S.; Ocheterski, J.; Petersson G. A.; Ayala, P. Y.; Cui, Q.; Morokuma, K.; Malik, D. K.; Rabul, A. D.; Raghavachari, K.; Foresman, J. B.; Cioslowski, J.; Ortiz, J. V.; Stefanov, B. B.; Liu, G.; Liashenko, A.; Piskorz, P.; Komaromi, I.; Gomperts, R.; Martin, R. L.; Fox D. J.; Keith, T.; Al-Laham, M. A.; Peng C. Y.; Nanayakkara, A.; Gonzalez, C.; Challacombe, M.; Gill, P. M. W.; Johnson, B. G.; Chem, W.; Wong, M. W.; Andres, J. L.; Head-Gordon, M.; Replogle, E. S.; Pople, J. A. *Gaussian 98*, revision A.3. Gaussian Inc.: Pittsburgh, PA, 1998.
(17) Stephens, P. J.; Devlin, F. J.; Chabalowski, C. F.; Frisch, M. J. *J. Phys. Chem.* **1994**, *98*, 11623−11627. Stephens, P. J.; Devlin, F. J.; Ashwar, C. S.; Chabalowski, C. F.; Frisch, M. J. *Faraday Discuss., Chem. Soc.* **1994**, *99*, 103−119.
(18) Petersson, G. A.; Bennett, A.; Tensfeldt, T. G.; Al-Laham, M. A.; Shirley, W. A.; Mantzaris, J. *J. Chem. Phys.* **1988**, *89*, 2193−2218.
(19) Peng, C.; Ayala, P. Y.; Schlegel, H. B.; Frisch, H. J. *J. Comput. Chem.* **1996**, *17*, 49−56. Ayala, P. Y.; Schlegel, H. B. *J. Chem. Phys.* **1997**, *107*, 375−384.
(20) Grimme, S.; Peyerimhoff, S. D. *Chem. Phys.* **1996**, *204*, 411−417.
(21) Janke, R. H.; Haufe, G.; Wùrthwein, E. U.; Borkent, J. H. *J. Am. Chem. Soc.* **1996**, *118*, 6031−6035.
(22) Martin, R. H.; Marchant, M. J. *Tetrahedron* **1974**, *30*, 347−349.
(23) Goedicke, Ch.; Stegemeyer, H. *Tetrahedron Lett.* **1970**, *12*, 937−940.
(24) Frisch, M. J.; Trucks, G. W.; Schlegel, H. B.; Scuseria, G. E.; Robb, M. A.; Cheeseman, J. R.; Montgomery, J. A., Jr.; Vreven, T.; Kudin, K. N.; Burant, J. C.; Millam, J. M.; Iyengar, S. S.; Tomasi, J.; Barone, V.; Mennucci, B.; Cossi, M.; Scalmani, G.; Rega, N.; Petersson, G. A.; Nakatsuji, H.; Hada, M.; Ehara, M.; Toyota, K.; Fukuda, R.; Hasegawa, J.; Ishida, M.; Nakajima, T.; Honda, Y.; Kitao, O.; Nakai, H.; Klene, M.; Li, X.; Knox, J. E.; Hratchian, H. P.; Cross, J. B.; Adamo, C.; Jaramillo, J.; Gomperts, R.; Stratmann, R. E.; Yazyev, O.; Austin, A. J.; Cammi, R.; Pomelli, C.; Ochterski, J. W.; Ayala, P. Y.; Morokuma, K.; Voth, G. A.; Salvador, P.; Dannenberg, J. J.; Zakrzewski, V. G.; Dapprich, S.; Daniels, A. D.; Strain, M. C.; Farkas, O.; Malick, D. K.; Rabuck, A. D.; Raghavachari, K.; Foresman, J. B.; Ortiz, J. V.; Cui, Q.; Baboul, A. G.; Clifford, S.; Cioslowski, J.; Stefanov, B. B.; Liu, G.; Liashenko, A.; Piskorz, P.; Komaromi, I.; Martin, R. L.; Fox, D. J.; Keith, T.; Al-Laham, M. A.; Peng, C. Y.; Nanayakkara, A.; Challacombe, M.; Gill, P. M. W.; Johnson, B.; Chen, W.; Wong, M. W.; Gonzalez, C.; Pople, J. A. *Gaussian 03*, Revision B.05, Gaussian Inc.: Pittsburgh, PA, 2003.
(25) The available CD data are found in 4 sources (refs 8, 9, 10, and 23) which all seem to derive from an original spectrum of Günther Snatzke, measured from material provided by the authors of ref 23. While the CD data are reported in ref 23, the CD spectrum first appears in ref 8, and subsequently in redrawn (to λ-linear) format in refs 9 and 10. Possibly due to scaling, the weak transitions at $\lambda > 309$ nm are not evident in the spectra of refs 9 and 10, and the $\Delta\epsilon$ values reported in ref 10 appear to be only half those of refs 8 and 9. The potential confusion now in the literature suggests that the CD spectrum of [5]helicene be remeasured.
(26) Cahn, R. S.; Ingold, C. K.; Prelog, V. *Angew. Chem., Int. Ed.* **1966**, *5*, 385−415.
(27) Gilbert, R. G.; Smith, S. C. *Theory of Unimolecular and Recombination Reactions*; Blackwell Scientific Publications: Oxford, England, 1990.
(28) Diedrich, C.; Grimme, S. *J. Phys. Chem. A* **2003**, *107*, 2524−2539. Parac, M.; Grimme, S. *Chem. Phys.* **2003**, *292*, 11−21.
(29) Ballhausen, R. G.; Hansen, A. E. *Annu. Rev. Phys. Chem.* **1972**, *23*, 15−38.
(30) Hansen A. E. Private communication.
(31) Platt, J. R. *J. Chem. Phys.* **1949**, *17*, 484−495.